Integral Piezoactuator System with Optimum Placement of Functionally Graded Material – A Topology Optimization Paradigm

RONNY C. CARBONARI,[1] GLAUCIO H. PAULINO[2,3] AND EMÍLIO C. N. SILVA[1,*]

[1]*Department of Mechatronics and Mechanical Systems Engineering, Escola Politécnica da Universidade de São Paulo, Av. Prof. Mello Moraes, 2231, 05508-900, São Paulo, SP, Brazil*

[2]*Newmark Laboratory, Department of Civil and Environmental Engineering, University of Illinois at Urbana-Champaign, 205 North Mathews Av., Urbana, IL, 61801, USA*

[3]*Department of Mechanical Science and Engineering, University of Illinois at Urbana-Champaign, 158 Mechanical Engineering Building, 1206 West Green Street, Urbana, IL 61801-2906, USA*

ABSTRACT: Piezoactuators consist of compliant mechanisms actuated by two or more piezoceramic devices. During the assembling process, such flexible structures are usually bonded to the piezoceramics. The thin bonding layer(s) between the compliant mechanism and the piezoceramic may induce undesirable behavior, including unusual interfacial non-linearities. This constitutes a drawback of piezoelectric actuators and, in some applications, such as those associated to vibration control and structural health monitoring (e.g., aircraft industry), their use may become either unfeasible or at least limited. A possible solution to this standing problem can be achieved through the functionally graded material concept and consists of developing 'integral piezoactuators', that is those with no bonding layer(s) and whose performance can be improved by tailoring their structural topology and material gradation. Thus, a topology optimization formulation is developed, which allows simultaneous distribution of void and functionally graded piezoelectric materials (including both piezo and non-piezoelectric materials) in the design domain in order to achieve certain specified actuation movements. Two concurrent design problems are considered, that is the optimum design of the piezoceramic property gradation, and the design of the functionally graded structural topology. Two-dimensional piezoactuator designs are investigated because the applications of interest consist of planar devices. Moreover, material gradation is considered in only one direction in order to account for manufacturability issues. To broaden the range of such devices in the field of smart structures, the design of integral Moonie-type functionally graded piezoactuators is provided according to specified performance requirements.

Key Words: actuator, optimization, piezoelectric, FGM, topology, optimization.

INTRODUCTION

PIEZOELECTRIC actuators offer significant promise in a wide range of applications in Engineering, specially in the field of smart structures where they are used for sensing, actuation, nanopositioning, and micromanipulation (Ishihara et al., 1996). For instance, piezoelectric actuators are applied to airplane-wing deformation control (Tzou and Tseng, 1990), atomic force microscope (AFM), and scanning tunneling microscopes (STM) for positioning the sample or the probe, respectively (Shim and Gweon, 2001), micromanipulation (Pérez et al., 2006), cell manipulation, and microsurgery (Eisinberg et al., 2001). These actuators usually consist of flexible structures (compliant mechanism) actuated by two or more piezoceramic devices. In the actuator assembly, these compliant mechanisms (usually made of aluminum or brass) are bonded to the piezoceramic. The thin bonding layer between the compliant mechanism and piezoceramic may cause an unusual non-linear behavior of the actuator due to the fact the strains are not properly transmitted from the piezoceramic to the compliant mechanism. This is a drawback of piezoelectric actuators that poses quality control problems in the piezoactuator industry – for some applications, the use of the piezoelectric actuator may become unfeasible or at least limited. This is the case of the aircraft industry, for example, where piezoelectric actuators are used for

*Author to whom correspondence should be addressed.
E-mail: ecnsilva@usp.br
Figures 3, 8, 10–11 and 14–16 appear in color online: http://jim.sagepub.com

1045-389X/10/16 1653–16 $10.00/0 DOI: 10.1177/1045389X10386129

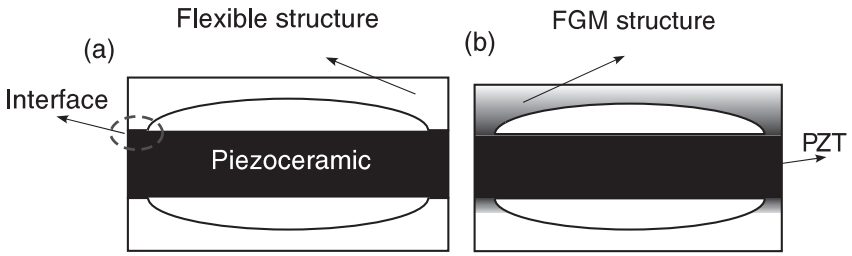

Figure 1. *(a) Conventional 'Moonie' piezoactuator with bonding layer and (b) Continuous 'Moonie' piezoactuator without bonding layer.*

vibration control and structural monitoring; however, the presence of bonding layers (the piezoactuators need to be bonded to the aircraft structure) reduces their reliability. However, a possible solution for this problem is the use of the functionally graded material technology, as illustrated in Figure 1.

Functionally graded materials (FGMs) are special materials that possess continuously graded properties and are characterized by spatially varying microstructures created by non-uniform distributions of the reinforcement phase as well as by interchanging the role of reinforcement and matrix (base) materials in a continuous manner (Miyamoto et al., 1999; Suresh, 2001). The smooth variation of properties may offer advantages such as local reduction of stress concentration and increased bonding strength. The concept of FGMs has been explored in piezoelectric materials to improve their properties and increase the lifetime of piezoelectric actuators (Almajid et al., 2001; Taya et al., 2003). Usually, elastic, piezoelectric, and dielectric properties are graded along the thickness of an FGM piezoceramic. Recently, a structurally graded (i.e., geometry) piezoelectric disc actuators was proposed by Heinonen et al. (2009).

Due to the attractive possibilities of tailoring the material properties, some researchers have applied optimization methods to design FGMs (see, for example, Turteltaub, 2002). The application of a generic optimization method, such as topology optimization, to design FGM piezoactuators has been presented by Carbonari et al. (2007a,b, 2009). In their works, optimization techniques have been applied to take advantage of the property gradation variation to improve the FGM piezoactuator performance, such as generated output displacements. However, the obtained FGM piezoactuator designs are either limited to simple shapes (Almajid et al., 2001; Taya et al., 2003; Carbonari, Silva and Paulino, 2007) or the FGM piezoceramic is kept fixed while only an attached compliant mechanism is designed (Carbonari et al., 2009).

The Integral Piezoactuator Concept

Functionally graded piezoelectric mechanisms can be defined as an FGM structure with complex topology made of piezoelectric and non-piezoelectric material that must generate output displacement and force at a certain specified point of the domain and direction. This approach offers as an advantage monolithic actuators with no bonding layers and whose performance can be improved by tailoring the topology and the FGM gradation. We will call the piezoactuators designed using this concept as integral piezoactuators. Thus, the development of these piezoelectric actuators requires the design of actuated compliant mechanisms (Howell, 2001) that can perform detailed specific movements taking into accout the coupling between movements generated by various piezoceramic regions. This objective can be achieved by means of topology optimization (Canfield and Frecker, 2000; Carbonari et al., 2005), which allows the simultaneous search for an optimal topology of a flexible structure as well as the optimal positions of the piezoceramic regions in the design domain, to achieve certain specified actuation movements (Buehler et al., 2004; Carbonari et al., 2007a).

Thus, the objective of this work is to develop a topology optimization formulation that allows the simultaneous distribution of void and FGM piezoelectric material (made of piezoelectric and non-piezoelectric material) in the design domain, to achieve certain specified actuation movements. To achieve designs that can be manufactured, a solution control technique is proposed which guarantees that piezoelectric material will occur in a continuous layer. This method allows the design of piezoelectric actuators without a bonding interface, which may be responsible for actuator nonlinear behavior. One-dimensional constraint of the FGM gradation is imposed to provide more realistic designs. Two design problems are considered simultaneously: the optimum design of the piezoceramic property gradation in the FGM piezoceramic domain, and the design of the FGM structural topology. Figure 2 illustrates the concept of the FGM piezoelectric devices proposed in this work. Initially, a design domain subjected to a constant and uniform electric field is defined. The objective is to distribute the FGM piezoelectric material (made of piezoelectric and non-piezoelectric material, such as aluminum, for example) and void to maximize the displacement at a certain location, as described in Figure 2(a). At the end of the

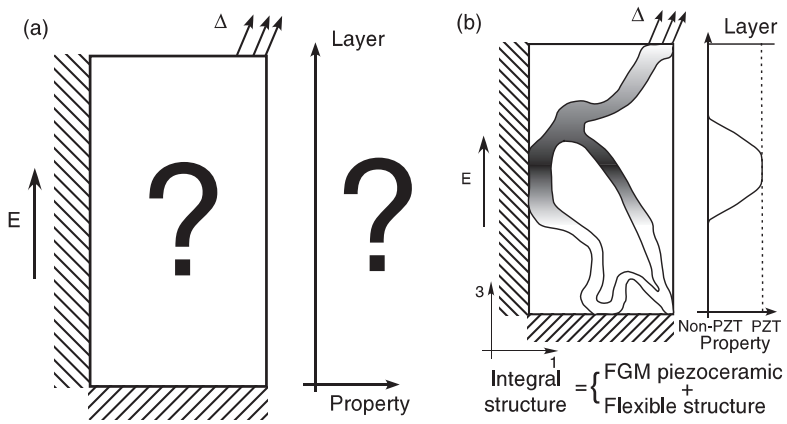

Figure 2. *(a) Design domain example to illustrate the concept of integral piezoelectric devices and (b) FGM piezoelectric device design considering the simultaneous distribution of integral piezoceramic and void in the design domain.*

optimization process, we expect to obtain not only the topology of the FGM structure, but also its material gradation. Both represent the concept of the 'integral structure', as described in Figure 2(b). For manufacturing purposes, a layering constraint is imposed to guarantee that the material gradation will occur in a continuous layer (only in one direction).

APPROACH

Topology optimization is a powerful structural optimization method that seeks an optimal structural topology design by determining which points of space should be solid and which points should be void (i.e., no material) inside a given domain (Bendsøe and Sigmund, 2003). However, the binary (0–1) design is an ill-posed problem and a typical way to seek a solution for topology optimization problems is to relax the problem by defining a material model that allows for intermediate (composites) property values. In this sense, the relaxation yields a continuous material design problem that no longer involves a discernible connectivity. Typically, it is an improperly formulated (ill-posed) topology optimization problem for which no optimum solution exists (0–1 design). A topology solution can be obtained by applying penalization coefficients to the material model to recover the 0–1 design (and thus, a discernible connectivity), and some gradient control of material distribution, such as a filter (Bendsøe and Sigmund, 2003; Belytschko et al., 2003).

However, the relaxed problem is strongly related to the FGM design problem, which essentially seeks a continuous transition of material properties (Miyamoto et al., 1999). In contrast, while the 0–1 design problem does not admit intermediate values of design variables, the FGM design problem does admit solutions with intermediate values of the material field.

Thus, in this study, the optimization problem is posed as the design of an FGM piezoelectric structure, as well as its property gradation that maximizes output displacement or output force in a specified direction and point of the domain, while minimizing the effects of movement coupling, as proposed by Carbonari et al. (2009). The method is implemented based on the solid isotropic material with penalization (SIMP) model where fictitious densities are interpolated at each finite element, providing a continuous material distribution in the domain. The optimization algorithm employed is based on sequential linear programming SLP (Hanson and Hiebert, 1981). Since the position of piezoceramic regions are not known 'a priori' an independent electrical excitation is considered for each finite element which is equivalent to a constant and uniformly applied electric field (Buehler et al., 2004; Carbonari et al., 2007a).

This design approach helps to tackle an important problem of piezoelectric actuators related to their nonlinear behavior due to the presence of a bonding interface. However, it is necessary to provide a design with defined and regular regions of piezoceramics for the sake of manufacturability.

This article is organized as follows. In the section 'Piezoelectric Finite Element FGM Modeling', a brief introduction about the numerical modeling of FGM piezoceramics considering, graded finite elements, is presented. In the section 'Design Problem Formulation', the continuous topology optimization method together with the adopted material model, and also the problem formulation of FGM piezoactuator design, are described. In the section 'Numerical Implementation', the design problem is discussed. In the section 'Projection of Material Distribution and Continuous Layering Constraint', a solution control technique which guarantees that piezoelectric material will occur in a continuous layer is given. In the section 'Numerical Results – Integral Piezoactuators', the design of an optimized integral Moonie-type piezoactuator is provided. Finally, some conclusions are inferred in the section 'Conclusion'.

PIEZOELECTRIC FINITE ELEMENT FGM MODELING

The integral piezoelectric actuators designed here operate in quasi-static or low-frequency environment where inertia effects can be ignored. When a non-piezoelectric conductor material and a piezoceramic material are distributed in the piezoceramic domain, the electrode positions are not known *a priori* (Carbonari et al., 2007a,b). Thus, the electrical excitation is given by an applied electric field ($\nabla\phi$ =constant). In this case, all electrical degrees of freedom are specified in the finite element problem, and thus, the weak formulation of the equilibrium equations of the piezoelectric medium considering linear piezoelectricity are given by (Carbonari et al., 2007a):

$$\begin{aligned}&\int_\Omega \varepsilon(\mathbf{u})^t \mathbf{c}^E \varepsilon(\mathbf{v})\mathrm{d}\Omega = \int_{\Gamma_t} \mathbf{t}\cdot\mathbf{v}\mathrm{d}\Gamma - \int_\Omega (\nabla\phi)^t \mathbf{e}^t \varepsilon(\mathbf{v})\mathrm{d}\Omega \\ &\int_\Omega \varepsilon(\mathbf{u})^t \mathbf{e}\nabla\varphi\mathrm{d}\Omega = \int_\Omega (\nabla\phi)^t \boldsymbol{\varepsilon}^S \nabla\varphi\mathrm{d}\Omega \\ &\text{for } \mathbf{u},\ \phi \in V \text{ and } \forall\mathbf{v},\ \forall\varphi \in V\end{aligned} \tag{1}$$

where

$$\mathbf{t} = \boldsymbol{\sigma}\cdot\mathbf{n};\ d = \mathbf{D}\cdot\mathbf{n} \tag{2}$$

are the mechanical traction and electrical charge, respectively, $\mathbf{n}$ is the normal vector to the surface and,

$$V = \{\mathbf{v} = v_i\bar{\mathbf{e}}_i,\ \varphi \text{ with } \mathbf{v} = 0 \text{ on } \Gamma_\mathbf{u} \text{ and } \varphi = 0 \text{ on } \Gamma_\phi, i = 1 \text{ or } 3\}$$

Ω is the domain of the medium (it may contain piezoelectric and non-piezoelectric materials), and ∇ the gradient operator. The superscript t denotes transpose, $\mathbf{v}$ and φ the virtual displacements and electric potential, respectively, $\mathbf{u}$ the displacement field, and ϕ the electric potential in the piezoelectric medium. The index i assumes value 1 or 3 because the problem is considered in the 1–3 plane. The piezoceramic is polarized in the local 3-direction.

The linear finite element matrix formulation of the equilibrium equations for the piezoelectric medium is given by (Lerch, 1990):

$$\begin{bmatrix}\mathbf{K_{uu}} & \mathbf{K_{u\phi}} \\ \mathbf{K_{u\phi}^t} & -\mathbf{K_{\phi\phi}}\end{bmatrix}\begin{Bmatrix}\mathbf{U} \\ \mathbf{\Phi}\end{Bmatrix} = \begin{Bmatrix}\mathbf{F} \\ \mathbf{Q}\end{Bmatrix} \Longrightarrow [\mathcal{K}]\{\mathcal{U}\} = \{\mathcal{Q}\} \tag{3}$$

where $\mathbf{K_{uu}}$, $\mathbf{K_{u\phi}}$, and $\mathbf{K_{\phi\phi}}$ denote the stiffness, piezoelectric, and dielectric matrices, respectively, and $\mathbf{F}$, $\mathbf{Q}$, $\mathbf{U}$, and $\mathbf{\Phi}$ are the nodal mechanical force, nodal electrical charge, nodal displacements, and nodal electric potential vectors, respectively (Lerch, 1990). Since $\mathbf{\Phi}$ is prescribed, the mechanical and electrical problems are decoupled, and only first Equation (4) needs to be directly solved, thus:

$$\begin{aligned}[\mathbf{K_{uu}}]\{\mathbf{U}\} &= \{\mathbf{F}\} - [\mathbf{K_{u\phi}}]\{\mathbf{\Phi}\} \\ [\mathbf{K_{u\phi}^t}]\{\mathbf{U}\} &= \{\mathbf{Q}\} + [\mathbf{K_{\phi\phi}}]\{\mathbf{\Phi}\}\end{aligned} \tag{4}$$

Essentially, the optimization problem is based on the mechanical problem and, as a consequence, the dielectric properties do not influence the design.

In the case of FGM piezoceramics, the properties change continuously inside the design domain, which means that they can be described by some continuous function of position $\mathbf{x}$ in the piezoceramic domain, that is:

$$\mathbf{c}^E = \mathbf{c}^E(\mathbf{x});\quad \boldsymbol{e} = \boldsymbol{e}(\mathbf{x});\quad \boldsymbol{\epsilon}^S = \boldsymbol{\epsilon}^S(\mathbf{x}). \tag{5}$$

From the mathematical definitions of $\mathbf{K_{uu}}$, $\mathbf{K_{u\phi}}$, and $\mathbf{K_{\phi\phi}}$, these material properties must remain inside the matrices integrals and be integrated together by using the graded finite element concept where properties are continuously interpolated inside each finite element based on property values at each finite element node. An attempt to approximate the continuous change of material properties by a stepwise function where a property value is assigned for each finite element may result in less accurate results with undesirable discontinuities of the stress and strain fields (Silva et al., 2007).

DESIGN PROBLEM FORMULATION

The topology optimization framework used in this study is based on the formulation for functionally graded piezoelectric actuators described in detail by Carbonari et al. (2007a). A continuum distribution of the design variable inside the finite element is considered through interpolation by means of continuous function which is obtained by defining the design variables related to the material distribution for each node which is called 'Continuous Approximation of Material Distribution' (CAMD) approach (Matsui and Terada, 2004). This formulation is fully compatible with the FGM concept (Carbonari et al., 2007b, 2009). We are interested in a simultaneous distribution of void, and FGM piezoelectric material in the design domain, and thus, the following material model is proposed based on an simple extension of the SIMP model (Bendsøe and Sigmund, 2003):

$$\mathbf{C}^H = \rho_1^p[\rho_2\mathbf{C}_1 + (1-\rho_2)\mathbf{C}_2] + \left(1-\rho_1^p\right)\mathbf{C}_{\text{void}} \tag{6}$$

$$\mathbf{e}^H = \rho_1^p[\rho_2\mathbf{e}_1 + (1-\rho_2)\mathbf{e}_2], \tag{7}$$

where ρ_1 and ρ_2 are pseudo-density function representing the amount of material at each point of the domain. These pseudo-density function can assume different values at each finite element node. Thus, $\rho_1 = 1.0$ denotes FGM material and $\rho_1 = 0.0$ is void, and $\rho_2 = 1.0$ denotes piezoelectric material type 1 and $\rho_2 = 0.0$ denotes piezoelectric material type 2 in the FGM material. $\mathbf{C}^H$ and $\mathbf{e}^H$ are stiffness and piezoelectric tensor properties, respectively, of the material. The tensors $\mathbf{C}_j$ and $\mathbf{e}_j$ are related to the stiffness and piezoelectric properties for piezoelectric material type j ($j = 1, 2$), respectively. $\mathbf{C}_{\text{void}}$ is the tensor related to void stiffness property. The piezoelectric material type 2 can be substituted by the flexible structure material (non-piezoelectric material, such as Aluminum, for example), and in this case $\mathbf{e}_2 = 0$. These are the properties of basic materials that are distributed in the piezoceramic domain.

The dielectric properties are not considered because a constant and uniform electric field is applied to the design domain as electrical excitation. This approach decouples the electrical and mechanical problems eliminating the influence of dielectric properties in the optimization problem. The p is a penalization factor to recover the discrete design, and its value varies from 0 to 3. For a discretized domain into finite elements, equations 6 and 7 are considered for each element node, and the material properties inside each finite element are given by functions of $\mathbf{x}$ ($\rho_1(\mathbf{x})$ and $\rho_2(\mathbf{x})$), where $\mathbf{x}$ denotes the Cartesian coordinates. This formulation leads to a continuous distribution of material along the design domain. Thus, by finding the nodal values of the unknown $\rho_1(\mathbf{x})$ and $\rho_2(\mathbf{x})$ function, we are indirectly finding the optimum material distribution functions, which are described by Equations (6) and (7).

The theoretical formulation for FGM piezoelectric actuator design by using topology optimization is described in detail by Carbonari et al. (2007b) and (2009); however, the simultaneous distribution of void and FGM piezoelectric material in the design domain is not considered. In this study, the goal is to design a device that generates the maximum output displacement considering a fixed design domain, however, the piezoceramic domain is not fixed and the piezoceramic electrodes are not known *a-priori*.

The objective function is defined in terms of generated output displacements for a certain applied electric field to the design domain which is related to the mean transduction ($L_2(\mathbf{u}_1, \phi_1)$) value (Silva et al., 2000). To provide enough stiffness for the piezoactuator, the mean compliance ($L_3(\mathbf{u}_3,\phi_3)$) must be minimized. In addition, to minimize undesired coupling displacements, a displacement coupling constraint is also considered by minimizing the absolute value of the corresponding mean transduction ($L_4(\mathbf{u}_1, \phi_1)$) related to the undesired generated displacement (Carbonari et al., 2009). This minimizes an undesired displacement generated when an electric field is applied.

To combine the mean transduction, mean compliance maximization, and coupling constraint minimization, a multi-objective function is constructed to find an appropriate optimal solution that can incorporate all design requirements. Thus, the following multi-objective function is adopted (Carbonari et al., 2009):

$$\mathcal{F}(\rho_1, \rho_2) = w * \ln[L_2(\mathbf{u}_1, \phi_1)] - \\ -\frac{1}{2}(1-w)\ln\left[L_3(\mathbf{u}_3, \phi_3)^2 + \beta L_4(\mathbf{u}_1, \phi_1)^2\right] \quad (8)$$

where w and β are weight coefficients ($0 \le w \le 1$, $\beta > 0$). The value of the coefficient w allows control of the contributions of mean transduction in relation to mean compliance and displacement coupling constraint function in the design. The value of β coefficient allows control of the contribution of coupling constraint function.

The final general optimization problem is defined as follows:

$$\begin{aligned}
&\text{Maximize:} && \mathcal{F}(\rho_1, \rho_2) \\
&\rho_1(\mathbf{x}),\ \rho_2(\mathbf{x}) && \\
&\text{subject to:} && a(\mathbf{u}_1, \mathbf{v}_1) + b(\phi_1, \mathbf{v}_1) = L_t(\mathbf{t}_1, \mathbf{v}_1) \\
& && b(\varphi_1, \mathbf{u}_1) - c(\phi_1, \varphi_1) = L_d(d_1, \varphi_1) \\
& && \text{for } \mathbf{u}_1, \phi_1 \in V_a \text{ and } \forall \mathbf{v}_1,\ \forall \varphi_1 \in V_a \\
& && a(\mathbf{u}_3, \mathbf{v}_3) + b(\phi_3, \mathbf{v}_3) = L_t(\mathbf{t}_3, \mathbf{v}_3) \\
& && b(\varphi_3, \mathbf{u}_3) - c(\phi_3, \varphi_3) = 0 \\
& && \text{for } \mathbf{u}_3, \phi_3 \in V_c \text{ and } \forall \mathbf{v}_3,\ \forall \varphi_3 \in V_c \\
& && 0 \le \rho_1(\mathbf{x}) \le 1 \\
& && 0 \le \rho_2(\mathbf{x}) \le 1 \\
& && \Theta_1(\rho_1) = \int_S \rho_1 \mathrm{d}S - \Theta_{1S} \le 0 \\
& && \Theta_2(\rho_2) = \int_{S_{PZT}} \rho_2 \mathrm{d}S - \Theta_{2S} \le 0
\end{aligned} \quad (9)$$

where:

$$a(\mathbf{u}, \mathbf{v}) = \int_\Omega \boldsymbol{\varepsilon}(\mathbf{u})^t \mathbf{c}^E \boldsymbol{\varepsilon}(\mathbf{v}) \mathrm{d}\Omega \qquad b(\phi, \mathbf{v}) = \int_\Omega (\nabla\phi)^t \mathbf{e}^t \boldsymbol{\varepsilon}(\mathbf{v}) \mathrm{d}\Omega$$
$$c(\phi, \varphi) = \int_\Omega (\nabla\phi)^t \boldsymbol{\varepsilon}^S \nabla\varphi \mathrm{d}\Omega \quad L_t(\mathbf{t}, \mathbf{v}) = \int_{\Gamma_t} \mathbf{t} \cdot \mathbf{v} \mathrm{d}\Gamma \quad (10)$$

and

$$V_a = \{\mathbf{v} = v_i \bar{\mathbf{e}}_i,\ \varphi \text{ with } \mathbf{v} = 0 \text{ on } \Gamma_u \text{ and } \nabla\varphi = \nabla\varphi_S \text{ in } \Omega,\ i = 1 \text{ or } 3\}$$
$$V_c = \{\mathbf{v} = v_i \bar{\mathbf{e}}_i,\ \varphi \text{ with } \mathbf{v} = 0 \text{ on } \Gamma_u, \text{ and } \varphi = 0 \text{ in } \Omega,\ i = 1 \text{ or } 3\}$$

Here S denotes the design domain, Θ_1 the constraint for FGM in the design domain, and Θ_{1S} the upper-bound constraint defined to limit the maximum amount of FGM in the design domain. Also, S_{PZT} denotes the FGM domain, Θ_2 the constraint for piezoceramic material in the FGM domain, and Θ_{2S} the upper-bound constraint defined to limit the maximum amount of piezoceramic in this domain. The other constraints are equilibrium equations for the piezoelectric medium (see section 'Piezoelectric Finite Element FGM Modeling') considering different load cases (Carbonari et al., 2007b, 2009). They are stated in the problem to indicate that, whatever topology is obtained, it must satisfy the equilibrium equations. The present notation follows closely the one by Bendsøe and Kikuchi (1988).

NUMERICAL IMPLEMENTATION

The continuum distribution of pseudo-density functions $\rho_1(\mathbf{x})$ and $\rho_1(\mathbf{x})$ are given by the function (Matsui and Terada, 2004; Rahmatalla and Swan, 2004):

$$\rho_1(\mathbf{x}) = \sum_{I=1}^{n_d} \rho_{1I} N_I(\mathbf{x}) \tag{11}$$

$$\rho_2(\mathbf{x}) = \sum_{I=1}^{n_d} \rho_{2I} N_I(\mathbf{x}) \tag{12}$$

where ρ_{1I} and ρ_{2I} are nodal variables, N_I the finite element shape function that must be selected to provide non-negative values of the design variables, and n_d is the number of nodes at each finite element. The variable ρ_{1I} can assume different values at each node of the finite element. The additional variable $\rho_2(\mathbf{x})$ is assumed to be uniform for each layer of nodes, and in the discretized form, becomes the variable ρ_{2e}.

Due to the definition of Equations (11) and (12), the material property functions (Equations (6) and (7)) also have a continuum distribution inside the design domain. Thus, considering the mathematical definitions of the stiffness and piezoelectric matrices of Equation (3), the material properties must remain inside the integrals and be integrated together by means of the graded finite element concept (Silva et al., 2007).

By means of the finite element matrix formulation of equilibrium (Equation (3)), the mean transduction and the mean compliance can be calculated numerically using the following expressions (Carbonari et al., 2007b):

$$\begin{aligned} L_2(\mathbf{U}_1, \mathbf{\Phi}_1) &= \{\mathbf{U}_1\}^t\{\mathbf{F}_2\} + \{\mathbf{\Phi}_1\}^t\{\mathbf{Q}_2\} = \{\mathbf{U}_1\}^t\{\mathbf{F}_2\} \\ &= \{\mathbf{U}_1\}^t\left[\mathbf{K}_{\mathbf{u}\phi}\right]\{\mathbf{\Phi}_2\} - \{\mathbf{\Phi}_1\}^t\left[\mathbf{K}_{\phi\phi}\right]\{\mathbf{\Phi}_2\} \end{aligned} \tag{13}$$

$$\begin{aligned} L_3(\mathbf{U}_3, \mathbf{\Phi}_3) &= \{\mathbf{U}_3\}^t\{\mathbf{F}_3\} + \{\mathbf{\Phi}_3\}^t\{\mathbf{Q}_3\} = \{\mathbf{U}_3\}^t\{\mathbf{F}_3\} \\ &= \{\mathbf{U}_3\}^t[\mathbf{K}_{\mathbf{uu}}]\{\mathbf{U}_3\} + \{\mathbf{U}_3\}^t\left[\mathbf{K}_{\mathbf{u}\phi}^t\right]\{\mathbf{\Phi}_3\} \end{aligned} \tag{14}$$

Note that $\{\mathbf{\Phi}_1\}^t\{\mathbf{Q}_2\} = 0$ (because $\{\mathbf{Q}_2\} = 0$) and $\{\mathbf{\Phi}_3\}^t\{\mathbf{Q}_3\} = 0$ (because $\{\mathbf{\Phi}_3\} = 0$) (Carbonari et al., 2007b, 2009). The expression for $L_4(\mathbf{U}_1, \mathbf{\Phi}_1)$ is equal to Equation (13) by substituting $\{\mathbf{F}_2\}$ by $\{\mathbf{F}_4\}$ and $\{\mathbf{Q}_2\}$ by $\{\mathbf{Q}_4\}$. The finite element equilibrium, Equation (3), is solved considering 4-node isoparametric finite elements under plane stress assumptions.

A relevant issue is how to define the piezoceramic electrodes. If non-piezoelectric and piezoelectric material are distributed in the design domain the position of the piezoceramic electrodes cannot be defined *a priori* because the piezoceramic location is not known in the design domain. To circumvent this problem, the electrical problem is considered independently for each finite element by defining a pair of electrodes at each finite element (Buehler et al., 2004; Carbonari et al., 2007a). Thus, each finite element has four electrical degrees of freedom given by $[\phi_a, \phi_b, \phi_c, \phi_d]$ (nodes are ordered counterclockwise starting from the upper right corner of each finite element) considering that one of the electrodes is grounded. Electrical voltage ϕ_0 is applied to the two upper nodes, and thus, the four electrical degrees of freedom are specified at each finite element as follows ($[\phi_0, \phi_0, 0, 0]$). This is equivalent to apply a constant electrical field along the 3-direction in the design domain.

PROJECTION OF MATERIAL DISTRIBUTION AND CONTINUOUS LAYERING CONSTRAINT

The CAMD approach ensures a continuous material distribution across elements. However, it does not provide a general control of the material distribution gradient. In previous works (Carbonari et al., 2007b, 2009), to achieve an explicit control of the material gradation, a technique based on projection functions (Guest et al., 2004; Carbonari et al., 2007b) was applied on top of CAMD, however, only for design variable ρ_2 considering horizontal layer design variable constraint, allowing gradation control. In this study, we apply the projection function based technique to both design variables ρ_1 and ρ_2 and continue assuming a horizontal layer design variable constraint for ρ_2 only. However, there is a more difficult challenge. When dealing with bulk FGMs, layered systems comprise the material of choice. However, when distributing FGM and void in the design domain, a result with alternated void and piezoelectric material in a same layer may occur, as described in Figure 3(a), which is very difficult to manufacture. It is desirable to have a continuous layer with piezoelectric material instead, as described in Figure 3(b). Thus, a layering constraint has been

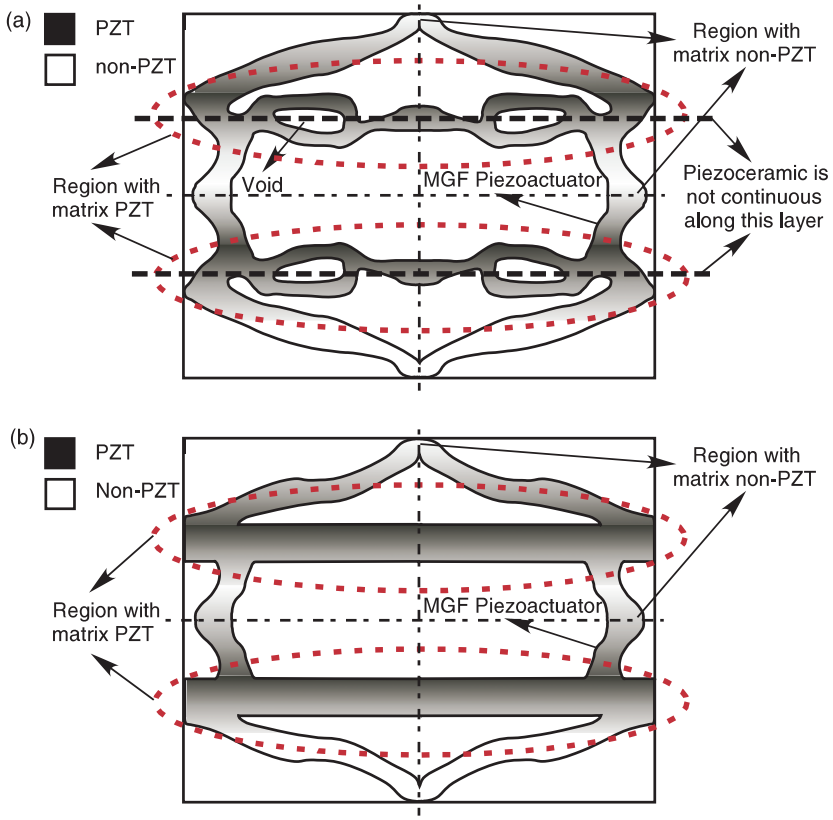

Figure 3. *(a) Design obtained without continuous layering constraint and (b) Design obtained considering continuous layering constraint.*

considered due to design and manufacturing reasons. From the design point of view, it is desirable to distribute the piezoceramic material through uniform horizontal layers to guarantee uniform poling of piezoceramic region. The polarization process requires high voltages – thus, if the piezoceramic region is distributed along horizontal layers of uniform thickness, then a uniform electric field is generated leading to uniform poling. Regarding the manufacturing issue, a good candidate for manufacturing the designed actuators (by means of topology optimization) is a sintering process based technique such as 'Spark Plasma Sinterin' (SPS). In this case, at first it is necessary to stack the material powders, which is easily achieved if horizontal layers of materials are considered. Thus, a new gradation control technique has been proposed to achieve this goal, as it will be described following.

Let d_n denote all design variables associated with nodes, and ρ_n (ρ_{2e} or ρ_{1i}), values of material density at nodes. Assume that the required change of material density must occur over a minimum length scale $r_{\min}$. By means of the projection function (f), ρ_{2e} can be obtained from d_{2j} as follows (assuming that four-node element is used):

$$\rho_{2e} = f(d_{2j}), \tag{15}$$

where e and j are layer numbers (Figure 4(b)) and f is the projection function defined as follows:

$$\rho_{2e} = f(d_{2j}) = \frac{\sum_{j\in S_e} d_{2j}\, W(r_{ej})}{\sum_{j\in S_e} W(r_{ej})}, \tag{16}$$

where r_{ej} are the distance between layers e and j given by:

$$r_{ej} = \|\mathbf{x}_j - \mathbf{x}_e\|. \tag{17}$$

and S_e is the set of layers in the design domain under influence of layers e, which consists in a strip of width r_{layer} centered at layer e. The weighting function $W(r_{ej})$ is defined as follows:

$$W(r_{ej}) = \begin{cases} \frac{r_{layer} - r_{ej}}{r_{layer}} & \text{if } \mathbf{x}_j \in S_e \\ 0 & \text{otherwise} \end{cases}, \tag{18}$$

Figure 4(a) illustrates the idea of this projection technique. As a consequence the topology optimization problem definition must be reviewed accordingly (Carbonari et al., 2007).

However, as discussed, it may occur that the piezoelectric material is not continuous along layer turning

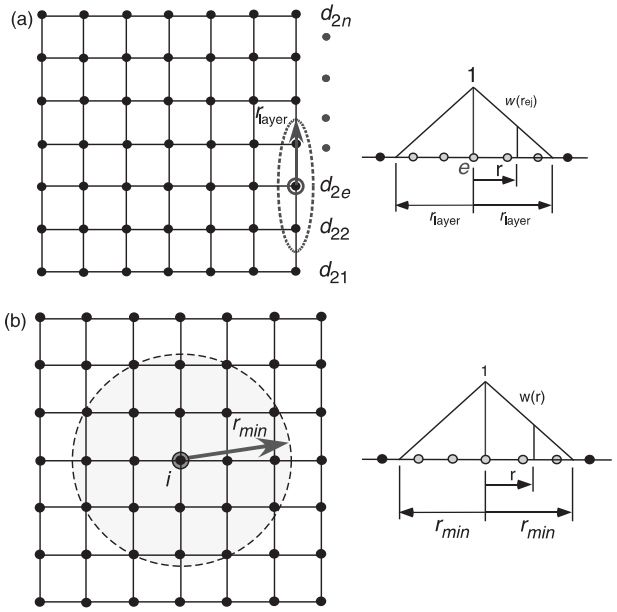

Figure 4. *Projection technique adapted to the CAMD concept. Notice that the projection cone is centered at a nodal point. (a) Nodal layer design variable ρ_{2e} and (b) Nodal design variable γ_{1i}.*

the manufacturing and poling a difficult task. To address this problem, a continuous layering constraint formulation is added, that allows the control of FGM piezoceramic material distribution (ρ_{1i}) to obtain regular defined regions, through following equation:

$$\rho_{1i} = \rho_{2i} + (1 - \rho_{2i})\gamma_{1i}, \tag{19}$$

where

$$\gamma_{1i} = f(d_{1j}), \tag{20}$$

and f is the projection function defined as follows:

$$\gamma_{1i} = f(d_{1j}) = \frac{\sum_{j \in S_i} d_{1j}\, H(r_{ij})}{\sum_{j \in S_i} H(r_{ij})}, \tag{21}$$

where r_{ij} is the distance between nodes j and i given by:

$$r_{ij} = \left\| \mathbf{x}_j - \mathbf{x}_i \right\|, \tag{22}$$

and S_i is the set of nodes in the design domain under influence of node i, which consists in a circle of radius r_{ij} centered at node i. The weighting function $H(r_{ij})$ is defined as follows:

$$H(r_{ij}) = \begin{cases} \frac{r_{\min} - r_{ij}}{r_{\min}} & \text{if } \mathbf{x}_j \in S_i \\ 0 & \text{otherwise} \end{cases}. \tag{23}$$

Figure 4(b) illustrates the idea of this projection technique.

These equations can guarantee the existence of material along the entire layer when there is a strong presence of piezoceramic material, that is, when d_{2e} or ρ_{2e} are close to 1.0. In this situation, the design variable ρ_{1i} will assume a value to guarantee that that the entire layer will be made of piezoelectric material. In this way, by using this defined projection technique, an FGM graded in horizontal layers and void can be distributed in the design domain.

Thus, the discretized form of the final optimization problem is defined as follows:

$$\begin{aligned}
&\text{Maximize:} && \mathcal{F}(d_{1I}, d_{2e}) \\
&\quad d_{1I}, d_{2e} && \\
&\text{subject to:} && [\mathcal{K}_1]\{\mathcal{U}_1\} = \{\mathcal{Q}_1\} \qquad [\mathcal{K}_3]\{\mathcal{U}_3\} = \{\mathcal{Q}_3\} \\
&&& 0 \le d_{1I} \le 1 \qquad I = 1..NE \\
&&& 0 \le d_{2e} \le 1 \qquad e = 1..NN \\
&&& \sum_{I=1}^{NE} d_{1I} V_I - \Theta_{1S} \le 0 \\
&&& \sum_{e=1}^{NN} d_{2e} V_e - \Theta_{2S} \le 0
\end{aligned} \tag{24}$$

where V_I and V_e denote the volumes associated with each finite element node (which is equal to the finite element volume) and layer, respectively. The parameter NE denotes the number of nodes in the design domain, which is equal to the number of design variables d_{1I}, and NN the number of layers in the piezoceramic design domain, which is equal to the number of design variables d_{2e}. The matrices $[\mathcal{K}_1]$ and $[\mathcal{K}_3]$ are reduced forms of the matrix $[\mathcal{K}]$ considering non-zero and zero prescribed voltage degrees of freedom in the domain, respectively. The initial domain is discretized by finite elements and the design variables are the values of d_{1I} and d_{2e} defined at each node and at each node layer, respectively.

A flow chart of the optimization algorithm describing the steps involved is shown in Figure 5. The software was implemented using the C language. Mathematical programming using SLP is applied to solve the optimization problem, which is appropriate when there are a large number of design variables, and different objective functions and constraints (Vanderplaats, 1984). The linearization of the problem at each iteration requires the sensitivities (gradients) of the multi-objective function and constraints. These sensitivities depend on gradients of mean transduction and mean compliance functions in relation to d_{1I} and d_{2e} (derived in the Carbonari et al. (2007b)). It must be noticed, however, that the derivatives of ρ_{1i} in relation to d_{1I} and d_{2e}, and ρ_{2e} in relation to d_{2e} must be included in the chain rule.

Suitable moving limits are introduced to assure that the design variables do not change by more than 5–15% between consecutive iterations. A new set of design variables d_{1I} and d_{2e} are obtained after each iteration, and

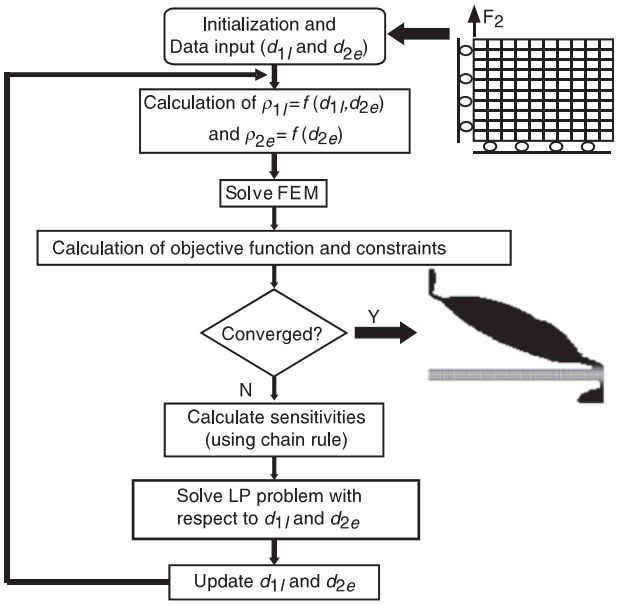

Figure 5. *Flow chart of optimization procedure (LP means linear programming).*

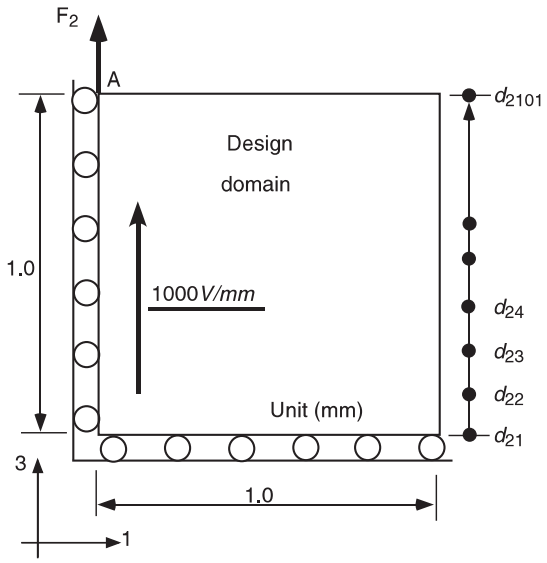

Figure 6. *Design domain for integral Moonie problem.*

Table 1. Material properties of piezoceramic PZT5A (Ikeda, 1996).

c^E_{11} (10^{10} N/m^2)	12.1	e_{13} (C/m^2)	−5.4
c^E_{12} (10^{10} N/m^2)	7.54	e_{33} (C/m^2)	15.8
c^E_{13} (10^{10} N/m^2)	7.52	e_{15} (C/m^2)	12.3
c^E_{33} (10^{10} N/m^2)	11.1		
c^E_{44} (10^{10} N/m^2)	2.30		
c^E_{66} (10^{10} N/m^2)	2.10		

the optimization continues until convergence is achieved for the objective function. The value of the penalization coefficient p is set equal from 1 to 3 following a continuation procedure (Carbonari et al., 2007).

NUMERICAL RESULTS – INTEGRAL PIEZOACTUATORS

Examples are presented to illustrate the design of integral piezoelectric actuators using the proposed method. Once the idea is to simultaneously distribute void, and FGM piezoelectric no regions with predefined materials are specified in the design domain S. For all examples, the FGM piezoelectric is composed of piezoelectric material and aluminum, and the material gradation is constrained to the 3-direction (Figure 6). Table 1 presents the piezoelectric material properties used in the simulations for all examples. $\mathbf{C}$ and $\mathbf{e}$ are the elastic and piezoelectric properties, respectively, of the medium. The Young's modulus and Poisson's ratio of aluminum are equal to 70 GPa and 0.33, respectively. $\mathbf{C}_{\text{void}}$ is equal to $10^{-10}\mathbf{C}_{\text{PZT}}$, where $\mathbf{C}_{\text{PZT}}$ is piezoelectric material stiffness tensor which terms are given by Table 1.

The design domain for all results is shown in Figure 6. This design domain is inspired in the design of the well-known 'Moonie' actuator (Onitsuka et al., 1995; Dogan et al., 1997), thus, we will call this design example as 'Integral Moonie'. Only one quarter of the actuator is designed by specifying symmetry conditions in the 1 and 3 axes. The adopted discretization for the design domain consists of 10,000 finite elements (rectangle discretized by a 100×100 elements or 101×101 nodes). The design domain is divided into 101 horizontal layers and design variable d_{2e} is considered for each layer, as described in Figure 6, while design variable d_{1I} is considered for each node. Thus, the number of design variables d_{1i} and d_{2e} are equal to 10,201, and 101, respectively. The mechanical and electrical boundary conditions are shown in Figure 6. For all examples, unless otherwise specified, the electric field applied to the design domain is equal to 1000 V/mm (Figure 6).

The objective consists of maximizing the output displacement at point A (Figure 6) along vertical direction. The initial value for design variables d_{1I} is equal to 0.05 in all cases, and for d_{2e} is equal to 0.05. Thus, the optimization problem starts in the feasible domain (all constraints satisfied). The pseudo-density variables ρ_{1I} and ρ_{2e} are obtained based on d_{1I} and d_{2e} using equations from 15 to 20. For each example, it is presented the topology of the integral piezoactuator and the FGM material gradation. The topology and material gradation results are shown by plotting the pseudo-density variables ρ_{1I}, and ρ_{2e} along layers, respectively. ρ_{1I} is plotted considering its average value inside each finite element.

It will be presented results with and without continuous layering constraint, in subsections

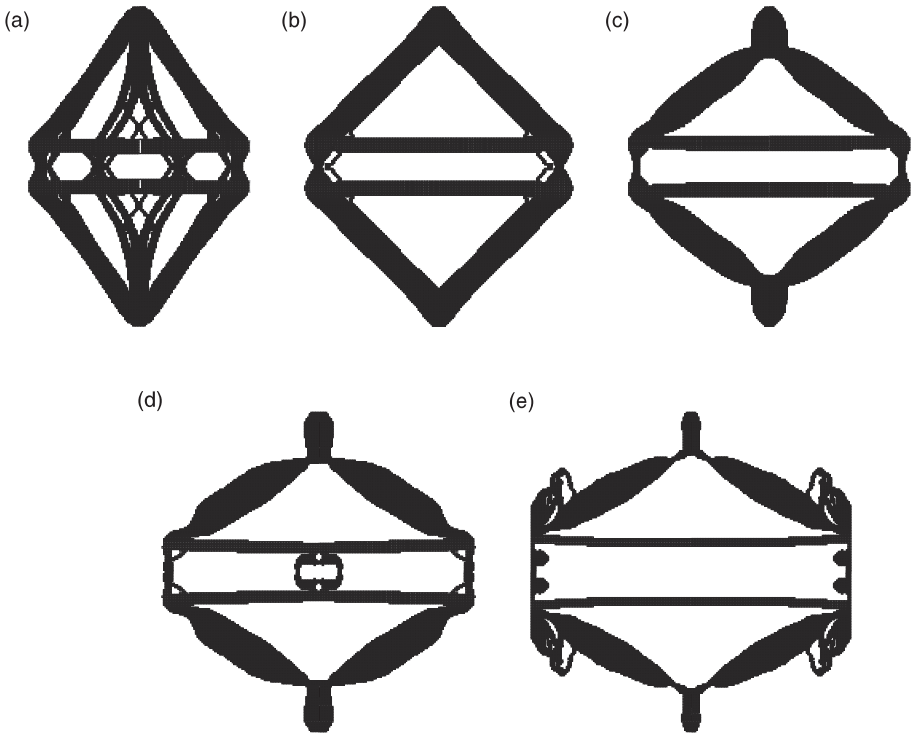

Figure 7. *Optimal topology of integral 'Moonie' obtained without continuous layering constraint: (a) w = 0.5, (b) w = 0.6, (c) w = 0.7, (d) w = 0.8, (e) w = 0.9.*

'Results Without Continuous Layering Constraint' and 'Results With Continuous Layering Constraint', respectively. For this example, due to the symmetry of the design domain, the coefficient β is equal to zero. In both approaches (with an without continuous layering constraint), the influence of value of coefficient w in the topology and gradation will be analyzed. The specified volume constraints for design variables d_{1I} and d_{2e} are equal to 25% and 10%, respectively. The projection technique are applied for design variable d_{1I} and d_{2e} considering a radius equal to 0.0011 mm ($r_{\min}$ involving four elements) and 0.0051 mm (r_{layer} involving five layers), respectively.

Table 2. Displacements at point A (1000V/mm applied).

MGF Moonie	u_y^* (nm)	u_y (nm)	w	layering constraint
Figure 8(a)	6.99	6.99	0.5	Without
Figure 14(a)	7.09	7.12	0.5	With
Figure 8(b)	13.04	13.01	0.6	Without
Figure 14(b)	15.02	14.95	0.6	With
Figure 8(c)	17.96	17.96	0.7	Without
Figure 14(c)	20.92	20.41	0.7	With
Figure 8(d)	26.16	25.89	0.8	Without
Figure 14(d)	23.93	24.07	0.8	With
Figure 8(e)	30.70	30.46	0.9	Without
Figure 14(e)	25.21	21.58	0.9	With

u_y^*: Result obtained for topology optimization.
u_y: Result obtained after post-processing.

Results Without Continuous Layering Constraint

At first, results without continuous layering constraint are presented in Figure 7, considering values for w ranging from 0.5 to 0.9. The deformed configurations are shown in Figure 8 and the displacement values in Table 2. The entire integral piezoactuator is plotted. It is interesting to notice that the optimized result for all examples are two well-defined regions of piezoceramic considering the entire actuator with a continuous transition from piezoceramic to aluminum. By analyzing these results, we verify that for a large value of w, the topology reaches the design domain boundaries, generating a larger output displacement for the actuation movement. Thus, for w equal to 0.5 a more compact, and thus, a more rigid structure, is obtained as expected. For w equal to 0.9, a more flexible structure is obtained with a piezoceramic region larger and narrower. Finally, for values of w larger than 0.7, the piezoceramic region becomes slightly curved, which is difficult to manufacture. In addition, Figure 9 shows a detail of some piezoactuator ends presented in Figure 7, where it can be noticed that the region with piezoelectric material has

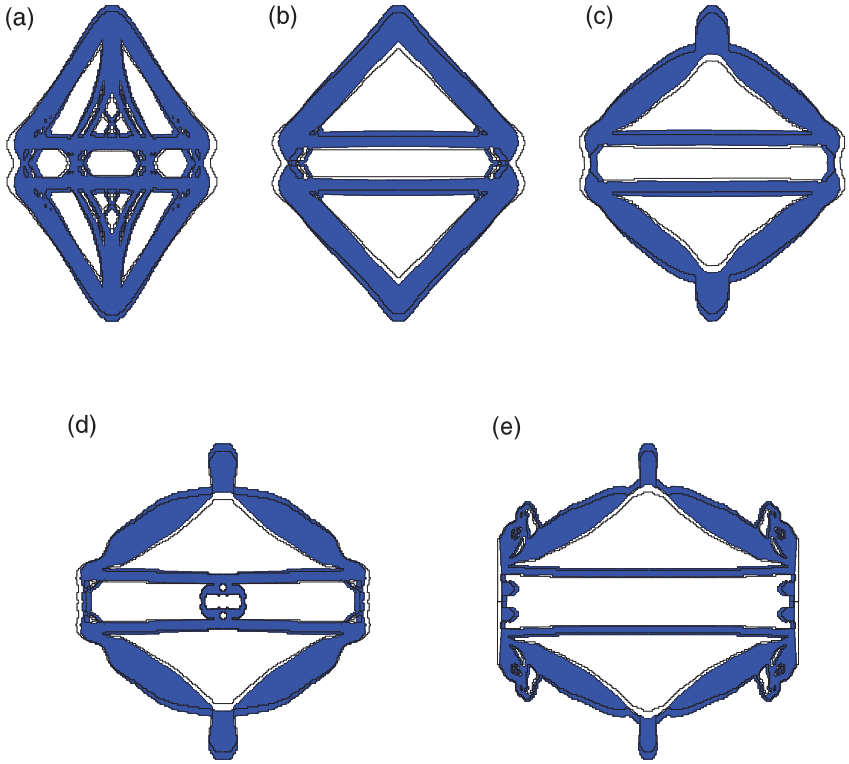

Figure 8. *Deformed configuration of post-processed topology obtained without continuous layering constraint (shaded — deformed shape; contour line — undeformed shape): (a) w = 0.5, (b) w = 0.6, (c) w = 0.7, (d) w = 0.8, (e) w = 0.9.*

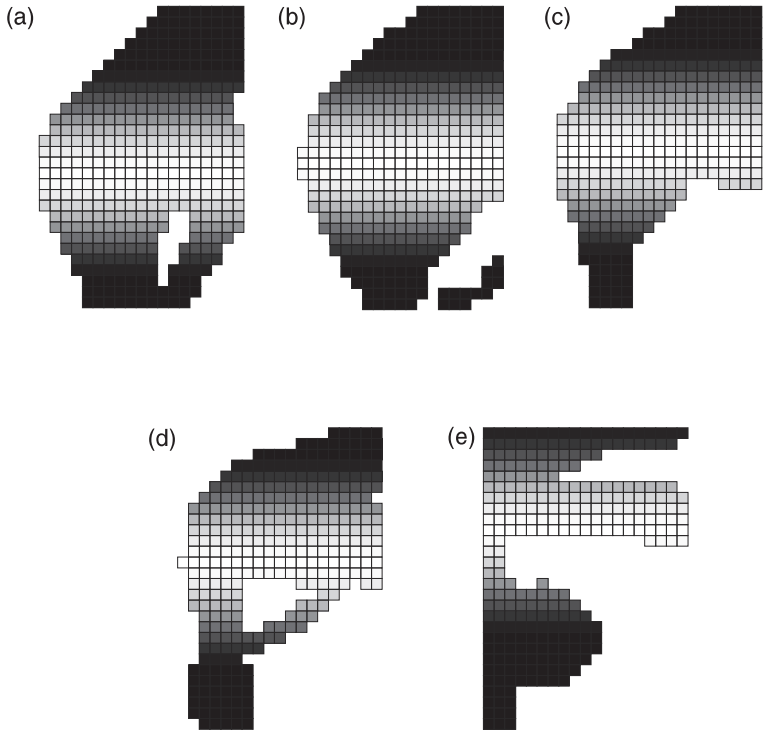

Figure 9. *Detail of the piezoactuator ends shown in Figure 7: (a) w = 0.5, (b) w = 0.6, (c) w = 0.7, (d) w = 0.8, (e) w = 0.9.*

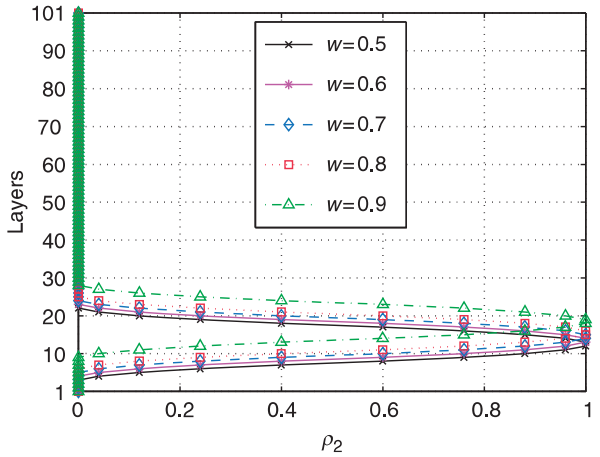

Figure 10. *Optimal ρ_{2e} values along layer numbers obtained without layering constraint by distributing piezoelectric and aluminum materials in the FGM domain.*

a rounded topology turning the manufacture a difficult task.

Now, by analyzing the material gradation (ρ_{2e}), as shown in Figure 10, we verify that for large values of w, the location of piezoelectric material changes, concentrating towards to the center of the domain. However, for all results the obtained gradation is symmetric in relation to the center line of piezoceramic region, as noticed by the plotted graphic points in Figure 10. The convergence graphics for multi-objective function, mean transduction, and mean compliance are plotted in Figure 11. The observed discontinuities are due to the continuation procedure adopted.

Results With Continuous Layering Constraint

These results, obtained using Equation 19, are presented in Figure 12, considering values for w ranging

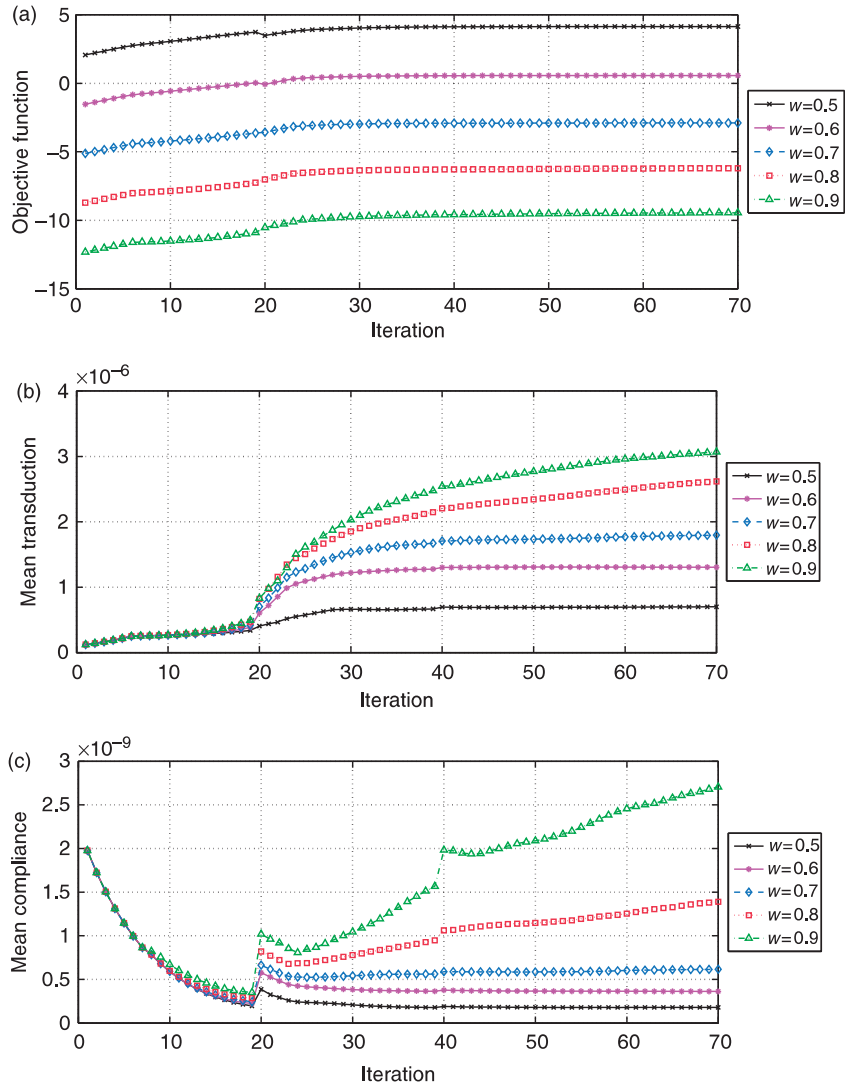

Figure 11. *Convergence graphics for results obtained without continuous layering constraint.*

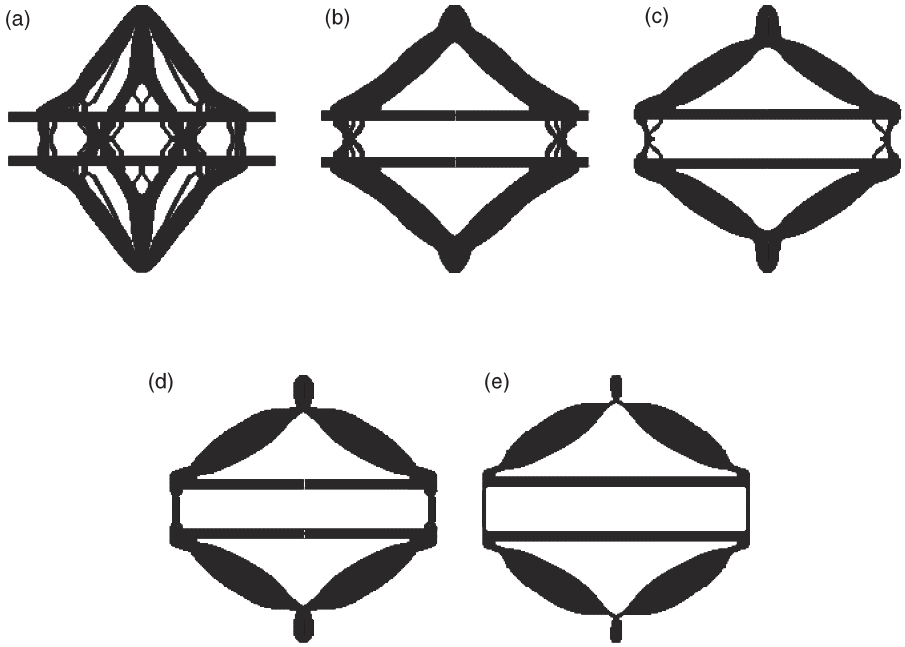

Figure 12. *Optimal topology of integral 'Moonie' obtained with continuous layering constraint: (a) w = 0.5, (b) w = 0.6, (c) w = 0.7, (d) w = 0.8, (e) w = 0.9.*

Figure 13. *Detail of the piezoactuator ends shown in Figure 12: (a) w = 0.5, (b) w = 0.6, (c) w = 0.7, (d) w = 0.8, (e) w = 0.9.*

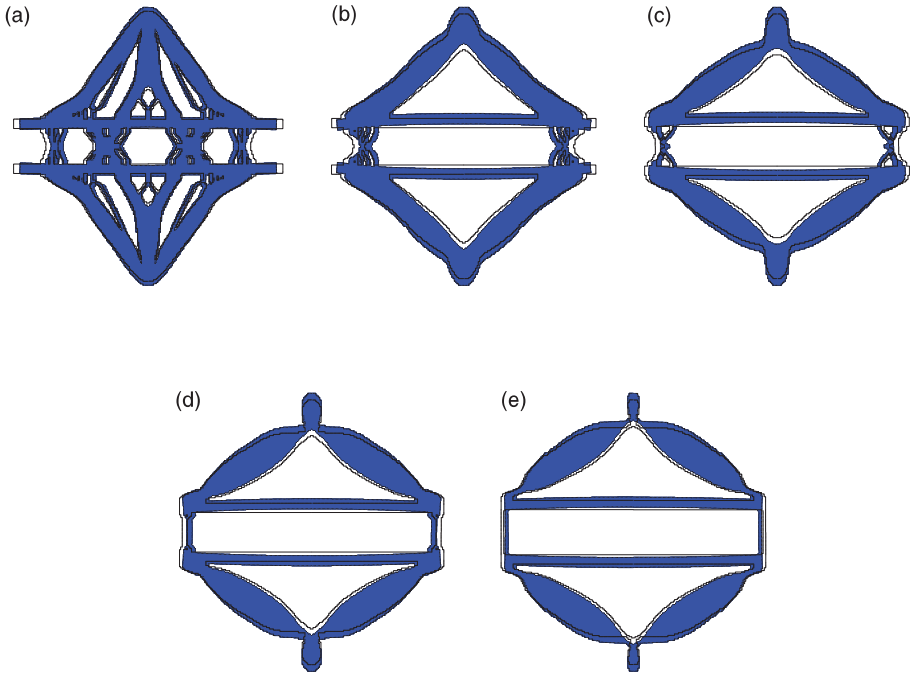

Figure 14. *Deformed configuration of post-processed topology obtained with continuous layering constraint (shaded — deformed shape; contour line — undeformed shape): (a) w = 0.5, (b) w = 0.6, (c) w = 0.7, (d) w = 0.8, (e) w = 0.9.*

from 0.5 to 0.9 (Figure 13). The deformed configurations are shown in Figure 14 and the displacement values are described in Table 2. The convergence graphics are plotted in Figure 15. The same optimization runs performed for results without continuous layering constraint are considered. The entire integral piezoactuator is plotted. The same comments for previous example apply for the topology results shown in Figure 12, including the symmetry obtained for the material gradation (ρ_2) in relation to the center line of piezoceramic region, as noticed by the plotted graphic points in Figure 16. However, a straight layer distribution is obtained for the piezoceramic instead. Notice that by eliminating the slightly curvature the displacement values for most flexible designs of Figure 14(d) and (e) decreased in relation to same designs of Figure 8(d) and (e). In addition, Figure 13 shows a detail of some piezoactuator ends presented in Figure 12, where it can be noticed that the problem reported in the previous example is less pronounced.

From Table 2, we notice that the post-processed displacement values for both examples, are close to the values obtained in the topology optimization result. Note that, as expected, the layering constraint reduces the optimality of the solution. Thus, for example, for small values of w (0.5, 0.6, and 0.7) less stiff actuator designs than designs without layering constraint are obtained (larger displacements are generated), and for large values of w (0.8 and 0.9) less flexible actuator designs than designs without layering constraint are obtained (smaller displacements are generated).

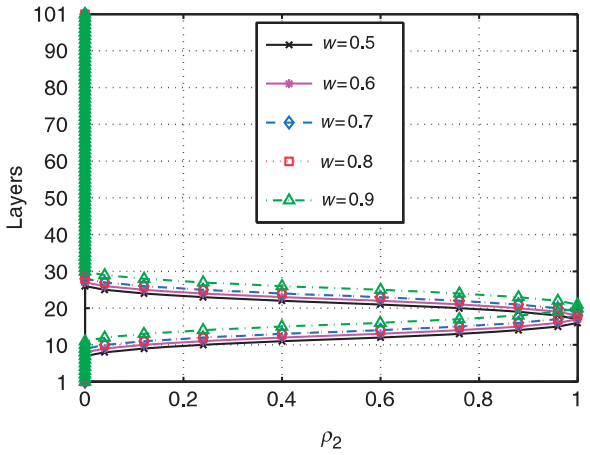

Figure 15. *Optimal ρ_{2e} values along layer numbers obtained with layering constraint by distributing piezoelectric and aluminum materials in the FGM domain.*

CONCLUSIONS

A topology optimization formulation has been proposed, which allows the implementation of the integral piezoactuator concept by searching for an optimal topology of an FGM piezoelectric structure that can achieve certain specified actuation movements. This is

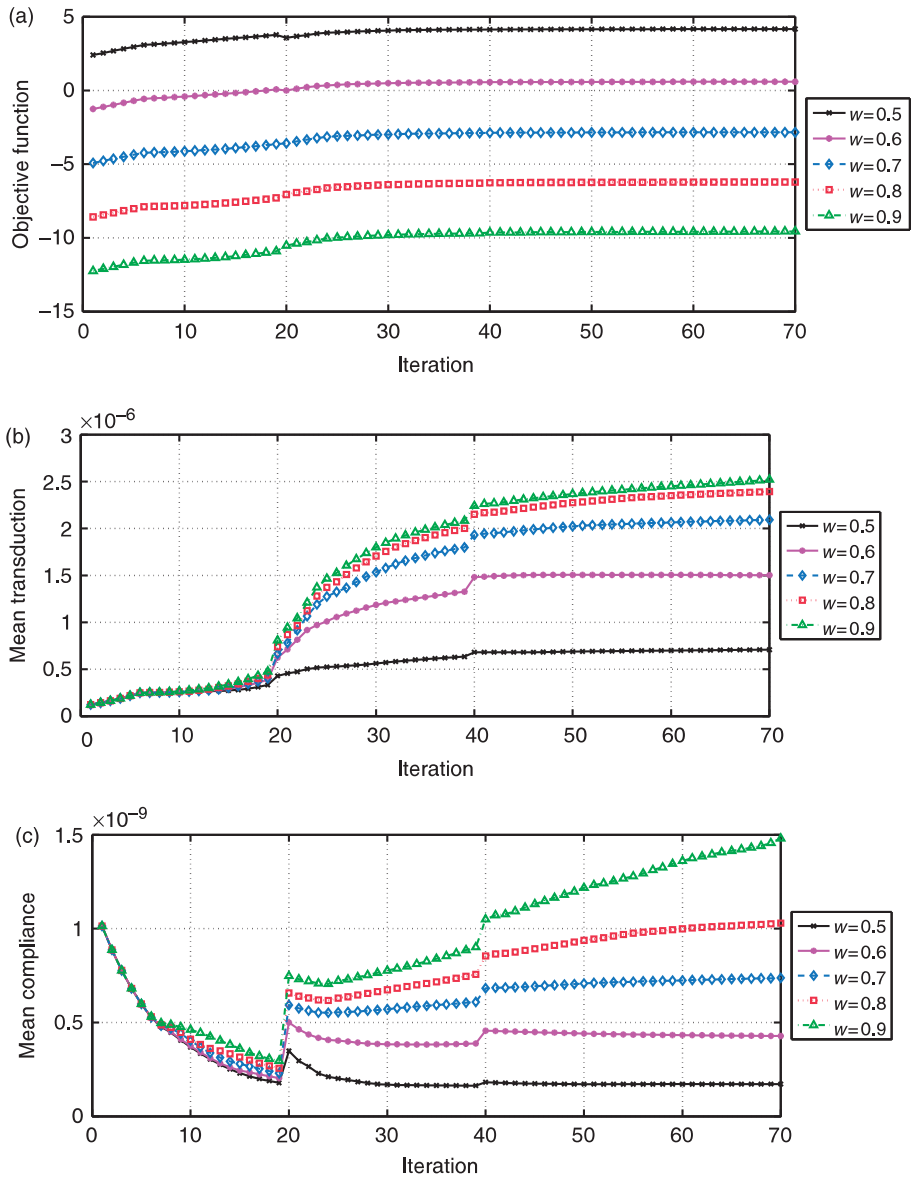

Figure 16. *Convergence graphics for results obtained with continuous layering constraint.*

achieved through optimization by allowing simultaneous distribution of void and graded piezoelectric material in the design domain, by finding the optimized location and gradation of FGM piezoceramics and holes in the design domain. Thus, this method allows the design of piezoelectric actuators without a bonding interface which may be responsible for undesirable actuator non-linear behavior. To achieve designs that can be manufactured, a solution control technique is proposed which guarantees that piezoelectric material will occur in a continuous layer. Some 2D plane stress examples are presented to illustrate the method and the efficacy of the solution control technique. We note that most of the applications for such FGM piezoactuators are planar devices. The obtained results are relevant for manufacturing. Thus, this formulation contributes to increase the design flexibility of these devices allowing the design of novel types of FGM piezoactuators without bonding layers for different applications, so called integral piezoactuators. The use of topology optimization for the design of integral piezoactuators has the potential to dramatically broaden the applied range of such devices, especially in the field of smart structures.

Our future work includes integration of analysis and manufacturing. For instance, the designed piezoelectric actuators will be manufactured in a mesoscale by using a SPS machine, and displacement measurements will be conducted to verify the performance of these designs.

ACKNOWLEDGMENTS

The author R. C. Carbonari would like to thank FUSP (University of São Paulo Foundation), for supporting him through a pos-doctoral fellowship. The author G. H. Paulino also thanks FAPESP for a visiting professor grant (n° 08/51070 – 0) at Polytechnic School of University of São Paulo (Brazil) during the second semester of 2008. The author Emílio C. N. Silva thanks FAPESP (Fundação de Amparo à Pesquisa do Estado de São Paulo), CNPq (project number n°s 303689/2009-9), and the University of Illinois at Urbana-Champaign (UIUC) for inviting him as a Visiting Professor during the Summer/2007.

REFERENCES

Almajid, A., Taya, M. and Hudnut, S. 2001. "Analysis of Out-of-plane Displacement and Stress Field in a Piezocomposite Plate with Functionally Graded Microstructure," *International Journal of Solids and Structures*, 38:3377–3391.

Belytschko, T., Xiao, S.P. and Parimi, C. 2003. "Topology Optimization with Implicit Functions and Regularization," *International Journal for Numerical Methods and Engineering*, 57:1177–1196.

Bendsøe, M.P. and Kikuchi, N. 1988. "Generating Optimal Topologies in Structural Design Using a Homogenization Method," *Computer Methods in Applied Mechanics and Engineering*, 71:197–224.

Bendsøe, M.P. and Sigmund, O. 2003. *Topology Optimization - Theory, Methods and Applications*, Springer, New York.

Buehler, M.J., Bettig, B. and Parker, G.G. 2004. "Topology Optimization of Smart Structures Using a Homogenization Approach," *Journal of Intelligent Mateial Systems Structures*, 15:655–667.

Canfield, S. and Frecker, M. 2000. "Topology Optimization of Compliant Mechanical Amplifiers for Piezoelectric Actuators," *Structures Multidisciplinary Optimization*, 20:269–279.

Carbonari, R.C., Silva, E.C.N. and Nishiwaki, S. 2005. "Design of Piezoelectric Multi-actuated Microtools Using Topology Optimization," *Smart Materials & Structures*, 14:1431–1447.

Carbonari, R.C., Silva, E.C.N. and Nishiwaki, S. 2007a. "Optimum Placement of Piezoelectric Material in Piezoactuator Design," *Smart Materials and Structures*, 16:207–220.

Carbonari, R.C., Silva, E.C.N. and Paulino, G.H. 2007b. "Topology Optimization Design of Functionally Graded Bimorph-type Piezoelectric Actuators," *Smart Materials and Structures*, 16:2605–2620.

Carbonari, R.C., Silva, E.C.N. and Paulino, G.H. 2009. "Multi-actuated Functionally Graded Piezoelectric Micro-tools Design: A Multiphysics Topology Optimization Approach," *International Journal For Numerical Methods In Engineering*, 77:301–336.

Dogan, A., Uchino, K. and Newnham, R.E. 1997. "Composite Piezoelectric Transducer with Truncated Conical Endcaps "Cymbal"," *IEEE Transactions on Ultrasonics Ferroelectrics and Frequency Control*, 44:597–605.

Eisinberg, A., Menciassi, A., Micera, S., Campolo, D., Carrozza, M. and Dario, P. 2001. "Pi Force Control of a Microgripper for Assembling Biomedical Microdevices," *IEE Proceedings of Circuits Devices System*, 148:348–352.

Guest, J.K., Prevost, J.H. and Belytschko, T. 2004. "Achieving Minimum Length Scale in Topology Optimization Using Nodal Design Variables and Projection Functions," *International Journal for Numerical Methods in Engineering*, 61:238–254.

Hanson, R. and Hiebert, K. 1981. "A Sparse Linear Programming Subprogram", Sandia National Laboratories, Technical Report SAND81-0297.

Heinonen, E., Juuti, J., Moilanen, V., Palosaari, J. and Jantunen, H. 2009. "Structurally Graded Monolithic Piezoelectric Actuators, Modeling and Optimization with FEM," *Journal of Intelligent Mateial Systems Structures*, 20:759–766.

Howell, L. 2001. *Compliant Mechanisms*, John Wiley & Sons, Inc., New York.

Ikeda, T. 1996. *Fundamentals of Piezoelectricity*, Oxford University Press, Oxford.

Ishihara, H., Arai, F. and Fukuda, T. 1996. "Micro Mechatronics and Micro Actuators," *IEEE/ASME Transactions on Mechatronics*, 1:68–79.

Lerch, R. 1990. "Simulation of Piezoelectric Devices by 2-dimensional and 3-dimensional Finiteelements," *IEEE Transactions on Ultrasonics Ferroelectrics and Frequency Control*, 37:233–247.

Matsui, K. and Terada, K. 2004. "Continuous Approximation of Material Distribution for Topology Optimization," *International Journal for Numerical Methods in Engineering*, 59:1925–1944.

Miyamoto, Y., Kaysser, W.A., Rabin, B.H., Kawasaki, A. and Ford, R.G. 1999. "*Functionally Graded Materials: Design*," *Processing and Applications*, Kluwer Academic Publishers, Dordrecht.

Onitsuka, K., Dogan, A., Tressler, J.F., Xu, Q., Yoshikawa, S. and Newnham, R.E. 1995. "Metal-ceramic Composite Transducer, the Moonie," *Journal of Intelligent Mateial Systems and Structures*, 6:447–455.

Pérez, R., Chaillet, N., Domanski, K., Janus, P. and Grabiec, P. 2006. "Fabrication, Modeling and Integration of a Silicon Technology Force Sensor in a Piezoelectric Micro-manipulator," *Sensors Actuators A-Physical*, 128:367–375.

Rahmatalla, S.F. and Swan, C.C. 2004. "A q4/q4 Continuum Structural Topology Optimization Implementation," *Structural and Multidisciplinary Optimization*, 27:130–135.

Shim, J.Y. and Gweon, D.G. 2001. "Piezo-driven Metrological Multiaxis Nanopositioner," *Review of Scientific Instruments*, 72:4183–4187.

Silva, E.C.N., Carbonari, R.C. and Paulino, G.H. 2007. "On Graded Elements for Multiphysics Applications," *Smart Materials & Structures*, 16:2408–2428.

Silva, E.C.N., Nishiwaki, S. and Kikuchi, N. 2000. "Topology Optimization Design of Extensional Actuators," *IEEE Transactions on Ultrasonics, Ferroelectrics and Frequency Control*, 47:657–671.

Suresh, S. 2001. "Graded Materials for Resistance to Contact Deformation and Damage," *Science*, 292:2447–2451.

Taya, M., Almajid, A.A., Dunn, M. and Takahashi, H. 2003. "Design of Bimorph Piezocomposite Actuators with Functionally Graded Microstructure," *Sensors and Actuators A-Physical*, 107:248–260.

Turteltaub, S. 2002. "Functionally Graded Materials for Prescribed Field Evolution," *Computer Methods in Applied Mechanics and Engineering*, 191:2283–2296.

Tzou, H.S. and Tseng, C.I. 1990. "Distributed Piezoelectric Sensor Actuator Design for Dynamic Measurement Control of Distributed Parameter-systems - a Piezoelectric Finite-element Approach," *Journal of Sound and Vibration*, 138:17–34.

Vanderplaats, G.N. 1984. *Numerical Optimization Techniques for Engineering Design: with Applications*, McGraw-Hill, New York.